hohlleiter zur geschirmten Streifenleitung mit homogenem sowie inhomogenem Dielektrikum," Ph.D. dissertation, Univ. of Bremen, Germany, 1976.
[13] G. Kowalski and R. Pregla, "Dispersion characteristics of shielded microstrips with finite thickness," *Arch. Elek. Ubertragung*, vol. 25, pp. 193–196, 1971.
[14] R. Mittra and T. Itoh, "A new technique for the analysis of the dispersion characteristics of microstrip lines," *IEEE Trans. Microwave Theory Tech.*, vol. MTT-19, pp. 47–56, 1971.
[15] H. J. Carlin, "A simplified circuit model for microstrip," *IEEE Trans. Microwave Theory Tech.*, vol. MTT-21, pp. 589–591, Sept. 1973.

Analysis of an End Launcher for an *X*-Band Rectangular Waveguide

MANOHAR D. DESHPANDE, MEMBER, IEEE, B. N. DAS, AND GITINDRA S. SANYAL

***Abstract*—The analysis of an end-laucher type, coaxial-to-rectangular waveguide transition, exciting dominant TE_{01} mode in *X*-band rectangular waveguide is presented. Expressions for the real and imaginary parts of the input impedance seen by the coaxial line are derived for the general case of an offset launcher using self-reaction of an assumed current over the loop. The dimensions of the combined electric and magnetic loops having low input VSWR in the coaxial line are determined. There is satisfactory agreement between theoretical and experimental results.**

I. Introduction

For the excitation of a two-dimensional array of rectangular waveguide radiators it is found convenient [1], [2] to use a colinear end-launcher transition from coaxial line-to-rectangular waveguide. Investigations on these types of transitions have been carried out by a number of workers. Wheeler [3] has empirically investigated the design of such a transition by matching the waveguide-to-coaxial line with the help of two step ridge transformers. Dix [4] also established a theoretical design procedure for the transition with a mixed four-section impedance transformer consisting of two ridged steps within the waveguide, one TEM section in the coaxial line, and a hybrid section where the coaxial center-conductor extends into the guide. A theoretical analysis for the design of a transition consisting of an L-shaped concentric loop without any additional impedance transformer has been presented by Das and Sanyal [5]. In their design, the dimensions of the L-shaped loop were selected in such a way that the real part of the input impedance seen by the coaxial line was equal to characteristic impedance of the coaxial line. The input reactance cancellation was achieved by a trial and error method. The bandwidth of the transition was very narrow. The maximum input VSWR of the transition was found to be 1.4 over the frequency range 9.2–9.5 GHz (300 MHz). The bandwidth of this type of transition can be more accurately determined, and a method of its improvement can be found if the explicit expressions for both real and imaginary parts of the input impedance seen by the coaxial line in terms of loop dimensions L_1, a', and b' (Fig. 1) are known.

In this paper, a more general analysis applicable to concentric as well as offset launcher in the form of an L-shaped loop placed in a dominant TE_{01}-mode rectangular waveguide is presented. The expressions for both the real and imaginary parts of input impedance seen by the coaxial line are derived from the self-reaction of an assumed current over the probe. The expression for the real part of input impedance is then used to find the loop dimensions L_1, a', and b' which give the real part of input impedance to be equal or close to characteristic impedance of the coaxial line over a range of frequencies. The variation of input reactance for these loop dimensions is computed as a function of frequency. From the variation of input impedance, the loop dimensions L_1, a', and b' which give low input VSWR in the coaxial line over a range of frequencies are determined. Theoretical and experimental results for input VSWR are compared for a transition with $L_1 = 1.4$ cm, $a' = 0.4$ cm, $b' = 1.15$ cm, and the probe diameter $2R = 0.2$ cm.

II. Analysis

Fig. 1(a) shows an L-shaped loop placed in a dominant TE_{01}-mode rectangular waveguide and driven from a generator through a coaxial line. The input impedance seen by the coaxial line driving the L-shaped loop is obtained from a stationary formula [6]:

$$Z_{\text{in}}|_c = -\int_v \frac{\vec{E}\cdot\vec{J}}{I_{\text{in}}^2}\,dv \tag{1}$$

where $\vec{E}$ is the electric field inside the guide due to

Manuscript received June 14, 1978; revised October 18, 1978.
The authors are with the Department of Electronics and Electrical Communications Engineering, Indian Institute of Technology, Kharagpur 721302, India.

0018-9480/79/0800-0731$00.75 ©1979 IEEE

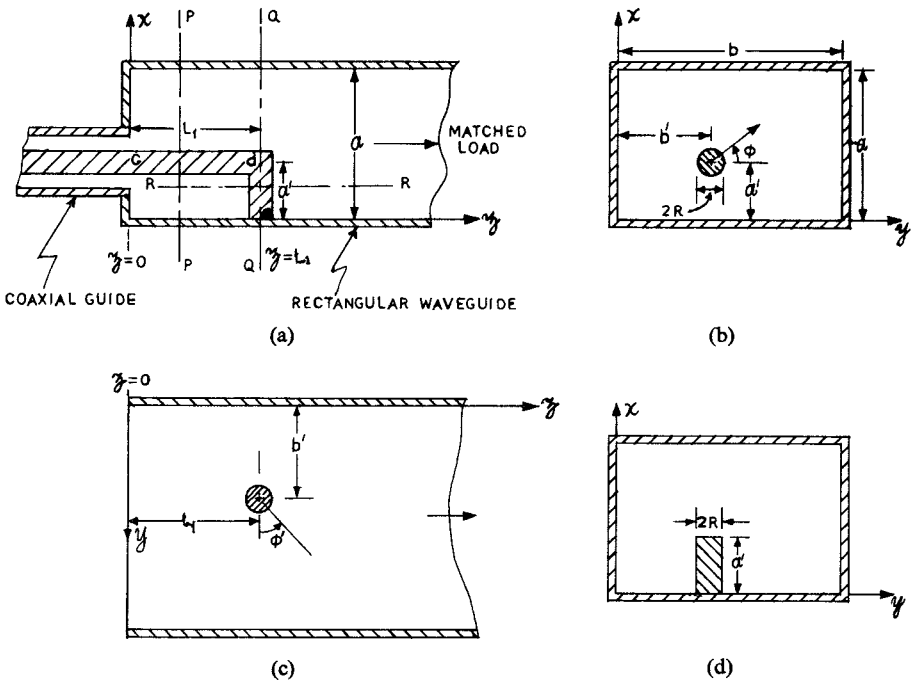

Fig. 1. An offset launcher for a rectangular waveguide terminated into matched load. (a) Longitudinal sectional view, *cde* L-shaped loop, *cd* —longitudinal arm, *de*—transverse arm. (b) Transverse sectional view at plane *PP*. (c) Longitudinal sectional view at plane *RR*. (d) Transverse sectional view at plane *QQ*.

current, $\vec{J}$ is distributed in the volume V, and I_{in} is the total input current at the reference point c (Fig. 1(a)). If $\vec{E}_{cd}$ is the electric field due to current, $\vec{J}_{cd}$ in the longitudinal arm cd of the loop, and $\vec{E}_{de}$ is the electric field due to current, $\vec{J}_{de}$ in the transverse arm de of the loop, (1) then takes the form:

$$Z_{\text{in}}|_c = -\int_v \frac{E_{cd}\cdot J_{cd}}{I_{\text{in}}^2}\,dv - \int_v \frac{E_{de}\cdot J_{de}}{I_{\text{in}}^2}\,dv. \tag{2}$$

In view of the stationary character of the above formula, the current distributions $\vec{J}_{cd}$ and $\vec{J}_{de}$ may be assumed of the form [5]:

$$\vec{J}_{cd} = \vec{a}_z j_{cd} = \vec{a}_z \frac{I_0}{2\pi R}\cos(K(L_1 + a' - z))\delta(x-(a'+R\sin\phi)) \cdot\delta(y-(b'+R\cos\phi)), \qquad \text{for } 0\leqslant z\leqslant L_1 \tag{3}$$

$$\vec{J}_{de} = \vec{a}_x j_{de} = \vec{a}_x \frac{I_0}{2\pi R}\cos(Kx)\delta(y-(b'+R\cos\phi')) \cdot\delta(z-(L_1+R\sin\phi')), \qquad \text{for } 0\leqslant x\leqslant a' \tag{4}$$

where $\vec{a}_x$ and $\vec{a}_z$ are the unit vectors along x and z axis, respectively, $2R$ is the diameter of cylindrical probe forming the L-shaped loop, the variables ϕ and ϕ' are as defined in Fig. 1(b) and (c), and $K=(2\pi/\lambda)$, λ being free-space wavelength. The field produced by z-directed current in the arm cd of the loop is given by [7]

$$\vec{H}_{cd} = \nabla\times\vec{A}_{cd}$$

$$\vec{E}_{cd} = -i\omega\mu\vec{A}_{cd} + \frac{1}{i\omega\epsilon}\nabla(\nabla\cdot\vec{A}_{cd}) \tag{5}$$

where the vector potential $\vec{A}_{cd}$ due to $\vec{J}_{cd}$ is

$$\vec{A}_{cd} = \vec{a}_z \sum_{n=1}^{\infty}\sum_{m=1}^{\infty} \frac{\sin\left(\frac{n\pi x}{a}\right)\sin\left(\frac{m\pi y}{b}\right)}{2ab\gamma} \cdot\int_v j_{cd}(x',y',z')\sin\left(\frac{n\pi x'}{a}\right)\sin\left(\frac{m\pi y'}{b}\right)e^{\pm\gamma(z-z')}dv. \tag{6}$$

The vector potential $\vec{A}_{de}$ due to x-directed current, $\vec{J}_{de}$ in the arm de of the loop is given by [7]

$$\vec{A}_{de} = \vec{a}_x \sum_{n=0}^{\infty}\sum_{m=1}^{\infty} \frac{\epsilon_n}{ab\gamma}\cos\left(\frac{n\pi x}{a}\right)\sin\left(\frac{m\pi y}{b}\right) \cdot\int_v j_{de}(x',y',z')\cos\left(\frac{n\pi x'}{a}\right)\sin\left(\frac{m\pi y'}{b}\right)e^{\pm\gamma(z-z')}dv. \tag{7}$$

The field inside the guide due to x-directed current is then obtained using (5) and (7) with subscript cd replaced by de. In (6) and (7) γ is the propagation constant in the waveguide, and is given by [7]

$$\gamma = \sqrt{\left(\frac{n\pi}{a}\right)^2 + \left(\frac{m\pi}{b}\right)^2 - K^2}\,. \tag{8}$$

The + and − signs in the exponentials appearing in (6) and (7) correspond to $z-z'<0$ and $z-z'>0$, respectively. The primed variables x', y', z' and the unprimed variables x, y, and z correspond to source and field points, respectively. $\epsilon_n = 1$ for $n=0$, and $\epsilon_n = 2$ otherwise. Since the current in the cylindrical conductor is distributed over its surface, the volume integrals reduce to surface integral. From (3), (4), (6), and (7) and considering that surface

element is $Rd\phi dz'$, expressions for the vector potentials are obtained in the form:

$$\vec{A}_{cd}=\vec{a}_z\sum_{n=1}^{\infty}\sum_{m=1}^{\infty}\frac{\sin\left(\frac{n\pi x}{a}\right)\sin\left(\frac{m\pi y}{b}\right)}{2ab\gamma}\cdot\int_0^{2\pi}\int_{-L_1}^{L_1}\frac{I_0}{2\pi}\cos(K(L_1+a'-|z'|))\delta(x'-(a'+R\sin\phi))\cdot\delta(y'-(b'+R\cos\phi))\sin\left(\frac{n\pi x'}{a}\right)\cdot\sin\left(\frac{m\pi y'}{b}\right)e^{\pm\gamma(z-z')}d\phi dz' \tag{9}$$

$$\vec{A}_{de}=\vec{a}_x\sum_{n=0}^{\infty}\sum_{m=1}^{\infty}\frac{e_n}{ab\gamma}\cos\left(\frac{n\pi x}{a}\right)\sin\left(\frac{m\pi y}{b}\right)\cdot\int_0^{a'}\int_0^{2\pi}\frac{I_0}{2\pi}\cos(Kx')\delta(y'-(b'+R\cos\phi'))\cdot\delta(z'-(L_1+R\sin\phi'))\cos\left(\frac{n\pi x'}{a}\right)\cdot\sin\left(\frac{m\pi y'}{b}\right)e^{\pm\gamma(z-z')}d\phi' dx'. \tag{10}$$

For calculating the vector potentials a first-order approximation [8] for a conductor of small radius can be made by putting $R=0$ in all terms, where the effect of R is very small. Thus terms of the form, $\sin(p\pi/a(a'+R\sin\phi))$ and $\cos(q\pi/b(b'+R\cos\phi))$ can be replaced by $\sin(p\pi a'/a)$ and $\cos(q\pi b'/b)$, respectively. Therefore, with a conducting plate at $z=0$ plane, the expression for the vector potentials in $z>0$ region is obtained from (9) and (10), as

$$\vec{A}_{cd}=\vec{a}_z\sum_{n=1}^{\infty}\sum_{m=1}^{\infty}\frac{I_0}{ab(K^2+\gamma^2)}\sin\left(\frac{n\pi a'}{a}\right)\cdot\sin\left(\frac{m\pi b'}{b}\right)\sin\left(\frac{n\pi x}{a}\right)\sin\left(\frac{m\pi y}{b}\right)\cdot\{\gamma\cos(K(L_1+a'-z))-e^{-\gamma L_1}\cdot[K\sin(Ka')+\gamma\cos(Ka')]\cdot\cosh(\gamma z)+Ke^{-\gamma z}\sin(K(L_1+a'))\} \tag{11}$$

and

$$\vec{A}_{de}=\vec{a}_x\sum_{n=0}^{\infty}\sum_{m=1}^{\infty}\frac{2I_0\epsilon_n K}{ab\gamma}\sin\left(\frac{m\pi b'}{b}\right)\cdot\sinh(\gamma L_1)\cos\left(\frac{n\pi x}{a}\right)\sin\left(\frac{m\pi y}{b}\right)e^{-\gamma z}\cdot\left\{\frac{\frac{n\pi}{Ka}\sin\left(\frac{n\pi a'}{a}\right)\cos(Ka')-\cos\left(\frac{n\pi a'}{a}\right)\sin(Ka')}{\left[K^2-\left(\frac{n\pi}{a}\right)^2\right]}\right\}. \tag{12}$$

The current j_{cd}, in the longitudinal arm cd, excites only higher order modes in the rectangular waveguide, while the current j_{de} in the transverse arm of the loop excites dominant as well as higher order modes. All higher order modes contribute to the reactive part of the input impedance.

In the evaluation of (2) assumption that $R\to 0$ cannot be made as it leads to a divergent series [8]. From (3), (5), and (11) the first term on the right-hand side of (2) is obtained as

$$-\iint_s\frac{\vec{E}_{cd}\cdot\vec{J}_{cd}}{I_{\text{in}}^2}ds=iX_1=i\sum_{n=1}^{\infty}\sum_{m=1}^{\infty}\frac{1}{2\pi\omega\epsilon ab\gamma}\cdot\frac{\sin\left(\frac{n\pi a'}{a}\right)\sin\left(\frac{m\pi b'}{b}\right)}{\cos^2(K(L_1+a'))}\cdot\int_0^{2\pi}\int_0^{L_1}[-e^{-\gamma L_1}\{K\sin(Ka')+\gamma\cos(Ka')\}\cdot\cosh\gamma z+Ke^{-\gamma z}\sin(K(L_1+a'))]\cdot\cos(K(L_1+a'-z))\cdot\sin\left(\frac{n\pi}{a}(a'+R\sin\phi)\right)\sin\left(\frac{m\pi}{b}(b'+R\cos\phi)\right)d\phi dz. \tag{13}$$

The functions $\sin(n\pi/a(a'+R\sin\phi))$ and $\sin(m\pi/b)(b'+R\cos\phi)$, appearing in the integrand, are expanded as product of sine and cosine functions. Expressing the functions $\sin(n\pi R/a)(\sin\phi)$, $\cos(n\pi R/a)(\sin\phi)$, $\sin(m\pi R/b)(\cos\phi)$, and $\cos(m\pi R/b)(\cos\phi)$ into Fourier–Bessel series and carrying out integration with respect to ϕ and also z, the expression for X_1 is obtained in the form:

$$iX_1=i\sum_{n=1}\sum_{m=1}\frac{120\pi}{KaKb}\frac{1}{\cos^2(K(L_1+a'))}\cdot F\frac{\sqrt{\left[\left(\frac{n\pi}{Ka}\right)^2+\left(\frac{m\pi}{Kb}\right)^2-1\right]}}{\left[\left(\frac{n\pi}{Ka}\right)^2+\left(\frac{m\pi}{Kb}\right)^2\right]}\cdot\left\{\sin^2\left(\frac{n\pi a'}{a}\right)\sin^2\left(\frac{m\pi b'}{b}\right)\left[J_0\left(\frac{n\pi R}{a}\right)J_0\left(\frac{m\pi R}{b}\right)\right]\right\} \tag{14}$$

where J_0 is the Bessel function of first kind, and

$$F=\left[e^{-\gamma L_1}\left\{\frac{K}{\gamma}\sin(Ka')+\cos(Ka')\right\}\cdot\left\{2\frac{K}{\gamma}\sin(K(L_1+a'))-\frac{K}{\gamma}\sin(Ka')\cosh(\gamma L_1)+\cos(Ka')\sinh(\gamma L_1)\right\}+\left(\frac{K}{\gamma}\right)^2\sin^2(K(L_1+a'))+\frac{K}{2\gamma}\sin(2K(L_1+a'))\right].$$

Similarly, from (4), (7), and (12) the second term on the right-hand side of (2) is obtained in the form:

$$-\int\int_s \frac{\vec{E}_{de}\cdot\vec{J}_{de}}{I_{in}^2}\,ds = i\sum_{n=0}\sum_{m=1}\frac{240\epsilon_n}{K^2ab}\frac{1}{(\gamma/K)}\cdot\frac{1}{\cos^2(K(L_1+a'))}\sin\left(\frac{m\pi b'}{b}\right)\cdot\frac{\left\{\frac{n\pi}{Ka}\sin\left(\frac{n\pi a'}{a}\right)\cos(Ka')-\cos\left(\frac{n\pi a'}{a}\right)\sin(Ka')\right\}^2}{\left[1-(n\pi/Ka)^2\right]}\cdot\int_0^{2\pi}\sin\left(\frac{m\pi}{b}(b'+R\cos\phi')\right)e^{-\gamma R\sin\phi'}d\phi'. \quad (15)$$

Separating the above expression into real and imaginary parts and reducing the double summation in the expression for imaginary part into single summation by the method suggested in the literature [9], (15) reduces to

$$-\int\int_s \frac{\vec{E}_{de}\cdot\vec{J}_{de}}{I_{in}^2}\,ds = R + i(X_2+X_3+X_4) \quad (16)$$

where

$$R=\frac{240\pi}{KaKb}\frac{\sin^2\left(\frac{\pi b'}{b}\right)\sin^2(Ka')}{\cos^2(K(L_1+a'))}\frac{\sin^2\left(KL_1\sqrt{\left[1-(\pi/Kb)^2\right]}\right)}{\sqrt{\left[1-(\pi/Kb)^2\right]}}\left[J_0\left(\frac{\pi R}{b}\right)J_0\left(KR\sqrt{\left[1-(\pi/Kb)^2\right]}\right)\right] \quad (16a)$$

$$X_2=\frac{120\pi}{KaKb}\frac{\sin^2\left(\frac{\pi b'}{b}\right)\sin^2(Ka')}{\cos^2(K(L_1+a'))}\frac{\sin\left(2KL_1\sqrt{\left[1-(\pi/Kb)^2\right]}\right)}{\sqrt{\left[1-(\pi/Kb)^2\right]}}\left[J_0\left(\frac{\pi R}{b}\right)J_0\left(KR\sqrt{\left[1-(\pi/Kb)^2\right]}\right)\right] \quad (16b)$$

$$X_3=\frac{120\pi}{Ka}\frac{\sin^2(Ka')}{\cos^2(K(L_1+a'))}\left\{\frac{1}{2}\log_e\left(\frac{2b}{\pi R}\right)\sin\left(\frac{\pi b'}{b}\right)-J_0\left(\frac{\pi R}{b}\right)\sin^2\left(\frac{\pi b'}{b}\right)+\frac{1}{2}\frac{K^2b^2}{\pi^2}\cos^2\left(\frac{Kb'}{b}\right)-\frac{K^2b^2}{4\pi^2}\left[\frac{(2\pi b'/b)^2}{2}\log_e\left(\frac{2\pi b'}{b}\right)-\frac{3}{4}\left(\frac{2\pi b'}{b}\right)^2-\frac{1}{288}\left(\frac{2\pi b'}{b}\right)^4\cdots\right]\right\} \quad (16c)$$

$$X_4=-\frac{120}{Ka\cos^2(K(L_1+a'))}\sum_{n=1}^{\infty}\frac{\left\{\frac{n\pi}{Ka}\sin\left(\frac{n\pi a'}{a}\right)\cos(Ka')-\cos\left(\frac{n\pi a}{a}\right)\sin(Ka')\right\}^2}{\left[(n\pi/Ka)^2-1\right]}\cdot\{K_0(K_nR)-K_0(2K_nb')\}. \quad (16d)$$

In the above expressions, X_2 is the reactance due to dominant mode, X_3 and X_4 are the reactances due to modes, with indexes $n=0, m>1$, and $n>0, m\geq 1$, respectively. K_0 in (16d) is the modified Bessel function of the second kind, and $K_n=\sqrt{\left[(n\pi/Ka)^2-1\right]}$. From (14) and (16) the total input impedance at the reference point "c" is obtained as

$$Z_{in}|_c = R_{in}+iX_{in}=R+i(X_1+X_2+X_3+X_4). \quad (17)$$

The input reflection-coefficient amplitude at the reference point c and the input VSWR in the coaxial line is determined through the relations

$$|\Gamma|=\frac{\sqrt{\left[(R_{in}-Z_{oc})^2+X_{in}^2\right]}}{\sqrt{\left[(R_{in}+Z_{oc})^2+X_{in}^2\right]}} \quad (18)$$

and

$$\text{VSWR}=\frac{1+(\Gamma)}{1-(\Gamma)} \quad (19)$$

where Z_{oc} is the characteristic impedance of the input coaxial line.

III. Results

The variation of real part of the input impedance is computed from (16a), and presented in Fig. 2 for L_1 and a' in the range $0.9\leq L_1\leq 1.4$ cm, $0.32\leq a'\leq 0.5$ cm, and $b'=1.15$ cm, $R=0.1$ cm. It is found from Fig. 2 that the real part of the input impedance crosses the 50-Ω line in the case of an offset launcher. Further, the real part of the input impedance is close to 50 Ω over a wide-frequency range for L_1 in the range $0.9\leq L_1\leq 1.4$ cm, $a'=0.4$ cm, and $b'=1.15$ cm. The reactive part of the input impedance is, therefore, calculated from (14) and (16b)–(d) for these dimensions of the loop. Single and double summations appearing in the expressions for reactances are rapidly convergent. The computed results on variation of input reactance with frequency are presented in Fig. 3. From Figs. 2(c) and 3 and using (18) and (19), the variation of input VSWR in the coaxial line for a launcher with $L_1=1.4$ cm, $a'=0.4$ cm, $b'=1.15$ cm, and probe diameter $=0.2$ cm is presented in Fig. 4 together with corresponding experimental data.

IV. Conclusion

The analysis of a L-shaped loop in a rectangular waveguide leads to the design of end-launcher type transition with low input VSWR over a wide frequency band. There is close agreement between theoretical and experimental results for input VSWR seen by the coaxial line. The minimum VSWR is 1.1, and it is less than 2.0 for frequencies in the range $9.2\leq f\leq 10.9$ GHz.

The concentric launcher ($a'=a/2=0.5$ cm, $b'=b/2=1.15$ cm) with L_1 adjusted for $R_{in}=50$ Ω gives high input

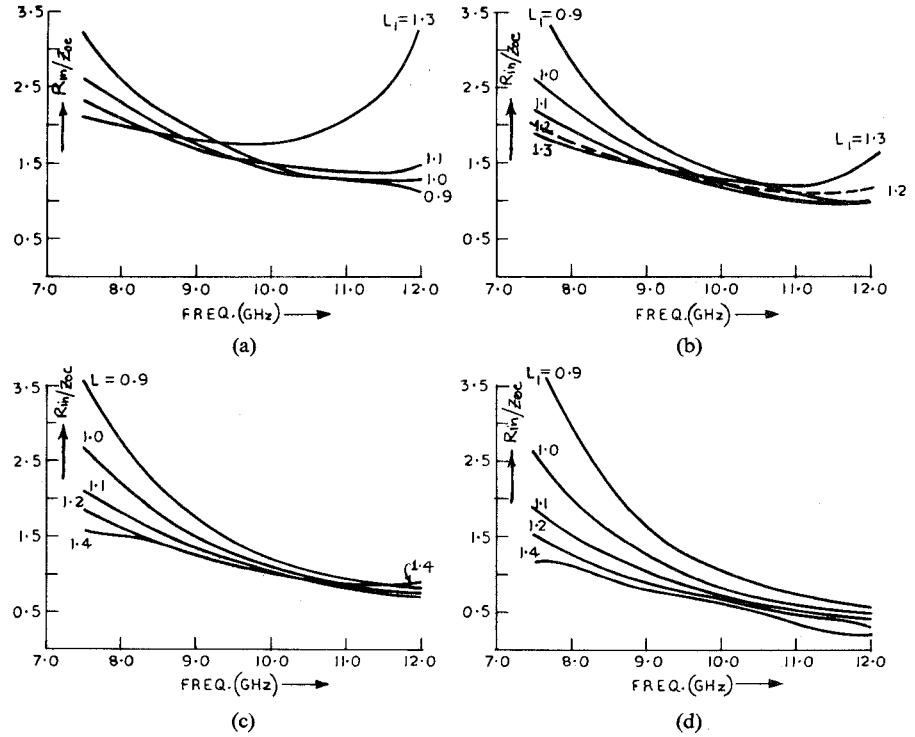

Fig. 2. Variation of real part of the input impedance versus frequency. (a) $a'=0.5$ cm, $b'=1.15$ cm (concentric). (b) $a'=0.45$ cm, $b'=1.15$ cm. (c) $a'=0.4$ cm, $b'=1.15$ cm. (d) $a'=0.32$ cm, $b'=1.15$ cm (offset launchers).

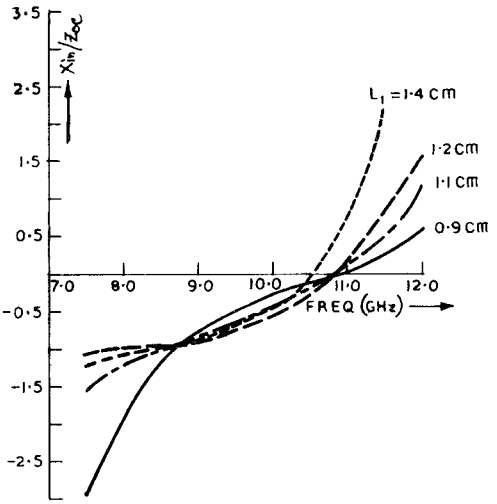

Fig. 3. Variation of imaginary part of the normalized input reactance versus frequency for $a'=0.4$ cm, $b'=1.15$ cm, $R=0.1$ cm.

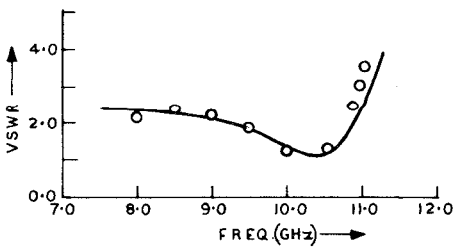

Fig. 4. Variation of input VSWR versus frequency for $a'=0.4$ cm, $b'=1.15$ cm, $R=0.1$ cm, $L_1=1.4$ cm. ——Theory, 0---0 Experimental.

reactance [5] and, therefore, needs additional arrangements for the input reactance cancellation. The results presented here show that the use of an offset launcher ($a'\neq a/2$, $b'=1.15$ cm) gives low input reactance which passes through zero at a frequency where the real part of the input impedance is close to 50 Ω. The offset launcher, therefore, does not require any additional arrangement for reactance cancellation. The low input reactance in the case of offset launcher can be attributed to the fact that as the launcher is displaced from axis of the waveguide the amplitudes of significant higher order modes decrease.

References

[1] Leo Young, Ed., *Advances in Microwaves*, vol. 4. New York: Academic, 1969, pp. 181–183.

[2] R. Tang and N. S. Wong, "Multimode phased array element for wide scan angle impedance matching," *Proc. IEEE*, vol. 56, pp. 1951–1959, Nov. 1968.

[3] G. J. Wheeler, "Broad band waveguide to coaxial transitions," *IRE Natl. Conv. Rec. 5, Pt. 1*, 1957, pp. 182–185.

[4] J. C. Dix, "Design of waveguide/coaxial transition for the band 2.5 to 4.1 GHz," *Proc. Inst. Elect. Eng.* (London), vol. 110, pp. 253–255, 1963.

[5] B. N. Das and G. S. Sanyal, "Coaxial to waveguide transition (end launcher type)," *Proc. Inst. Elec. Eng.*, vol. 123, no. 10, pp. 984–986, Oct. 1976.

[6] R. F. Harrington, *Time Harmonic Electromagnetic Fields*. New York: McGraw-Hill, 1961, ch. 8.

[7] G. Marcov, *Antennas*. Moscow, U.S.S.R.: Progress Publishers, 1965, ch. 2.

[8] L. Lewin, *Advanced Theory of Waveguides*. London, England: Eliffe & Sons, Ltd., 1951.

[9] R. E. Collin, *Field theory of Guided Waves*. New York: McGraw-Hill, 1960, ch. 7.